3rd URSI AT-AP-RASC, Gran Canaria, 29 May – 3 June 2022

A characteristic analysis of low-latitude NavIC signal intensity fading

Deepthi Ayyagari*(1) and Abhirup Datta(1)
(1) Department of Astronomy, Astrophysics and Space Engineering, IIT Indore, Madhya Pradesh -453552, India

Abstract

The current work for the first time aims to characterize the ionospheric scintillation on NavIC signals using Nakagami and $\alpha-\mu$ distribution as a representation of the fading effect. A clear depiction of the fading effect caused by scintillation on NavIC signals for an intense geomagnetic storm where the Dst Index has dropped to a minimum value of 124nT. The observed values of carrier to noise ratio (dB-Hz) for PRNs 2, 5 and 6 have dropped below 30 dB-Hz and have approached to value of zero between 22:00 to 0 LT(h). The severity of S_{4_c} index during that time peaked beyond the value of 0.5 as observed from PRN 2 of NavIC and the value of intensity fading that has reached up to -8dB. This paper lays the foundation for the intensity fading study of NavIC signals over region near EIA and another region near to magnetic equator on September 8, 2017.

1 Introduction

Ionospheric scintillations cause rapid changes in the phase and amplitude of the radio signal as it travels through the ionosphere. This phenomenon is dominant near equatorial regions ranging from -20^o to 20^o latitude and the auroral zone spanning from 55^o to 90^o latitude. It is difficult to predict and model ionospheric scintillations in the Equatorial ionization anomaly (EIA) regions due to the variability of many factors such as solar activity, interplanetary magnetic field conditions, local electric field, conductivity, convection processes, and wave interactions. Several researchers have used GPS data to study the phenomenon of ionospheric scintillation, as well as its causes and effects during extreme geomagnetic activity, over last few decades.[1]

2 Data and Locations of Observations

A multi-constellation, multi-frequency NavIC receiver provided by Space Applications Centre, ISRO, intercepting GPS L1, NavIC L5, and NavIC S1 (2492.028 MHz) signals, has been operational at DAASE in the Indian Institute of Technology, Indore, since May 2017. In addition to the NavIC data from the Indore (Lat:22.52^{o}N, Lon:75.92^{o}E; Magnetic dip:32.23^{o}N) station[2], the current study makes use of NavIC data from the Osmania University (OU), Hyderabad (Lat: 17.40^{o}N, Lon: 78.51^{o}E; Magnetic dip: 21.69^{o}N) station as shown in Figure1.

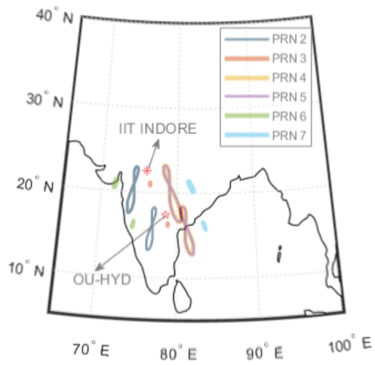

Figure 1. The geographic locations of the NavIC receivers along with the Ionospheric pierce points (IPPs) as observed from each of the locations

3 Scintillation Events: Selection Criteria

In support with NOAA scales, 27 days are selected out of 607 days analysed spanning from September 1, 2017 to September 30, 2019 for both the stations, based on the following[3, 4]:

1. The masking angle is set to 20^o to reduce multipath effects for elevation in the data sets and the S_{4_c} is filtered so that the threshold value for $S_{4_c} = 0.3$.
2. The event does not qualify as a scintillation event unless it remains above this threshold value for at least 30 seconds, and any event that begins within five minutes of the previous event is not treated as a separate event in order to avoid certain interference effects.
3. The S_{4_c} events observed from multiple satellites at the same time are analysed separately.
4. For the analysis, events with a loss-of-lock (LoL) lasting more than 120 seconds are considered.

The LoL is defined in this work as the receiver's ability to lose track of a transmitting satellite. For the duration of this time interval, the receiver will be unable to log any phase or pseudorange observations. Following the above criteria and analysing the entire 25 months of NavIC Indore observations, only 27 days qualify as scintillation events, i.e., only 4% of the nights in the total duration of the scintillations have been detected in the analysis, and these occurrences were chosen based on the distribution along the period of the study. In this paper we present the observational analysis a typical scintillation event occurred on September 8, 2017.

4 Analyzing and Characterizing: Amplitude Scintillation

On of the pre-dominant mechanisms which generate the amplitude scintillation in the equatorial and low latitude regions is the Pre-reversal Enhancement. This is generated as a result of the enhancement in the vertical E×B drift due to the eastward electric field at the sunset terminator generating Equatorial Plasma Bubble (EPB) and Equatorial Spread F (ESF) around this time[5]. The ionospheric TEC is derived by extracting ground-based observables from raw data files of NavIC. For each slant path between the satellite and the receiver, a slant TEC can be calculated with an assumption that the ionosphere is a thin shell (at 350 km altitude). The rate of change of slant TEC (ROT)10, provides an estimate of the ionospheric disturbances. In fact, a rate of slant TEC index that takes into account the average standard deviation of the rate of slant TEC. This index is defined as the Rate of TEC Index (ROTI)11[6, 7, 8, 13, 15]. In figures 2-3 (A to C) shows the onset times of amplitude scintillation S_{4_c}7to9 as observed from NavIC PRNs at L5 and S1 frequencies. The subplots (D to F) and (G to I) show the ROT and ROTI values as observed from the same satellites during time of occurrence of S_{4_c}. The (J to L) subplots in each of the figures 2-3 depict the variation of scattering coefficients[14] (S_{coeff})12 from the NavIC frequencies based on the deviations estimated from each PRN's at L5 and S1 respectively at both the locations.

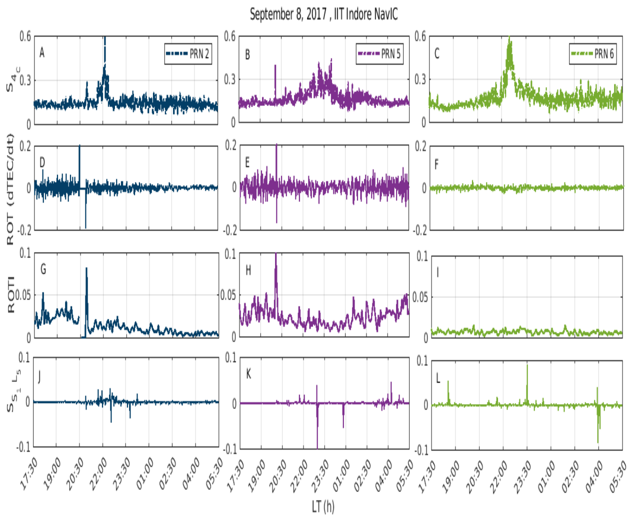

Figure 2. The S_{4_c}, ROT, ROTI and $S_{S_1 L_5}$ variation on September 8, 2017 as observed from Indore station during 17:30 LT (h) of September 8, 2017 to 05:30 LT (h) of September 9, 2017 for NavIC PRNs 2,5 and 6.

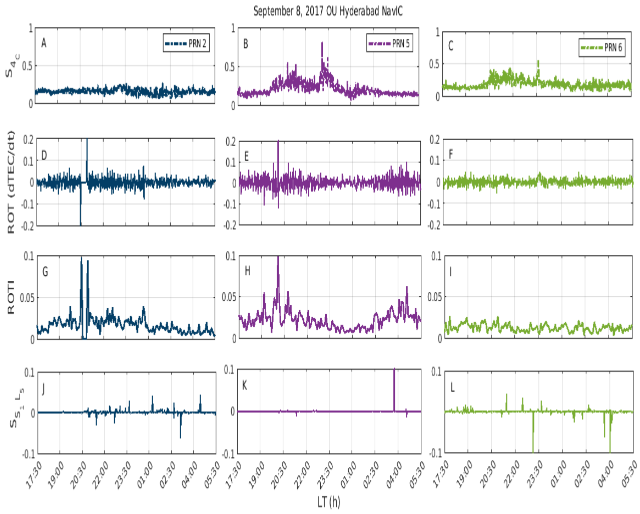

Figure 3. The S_{4_c}, ROT, ROTI and $S_{S_1}L_5$ variation on September 8, 2017 as observed from Hyderabad station during 17:30 LT (h) of September 8, 2017 to 05:30 LT (h) of September 9, 2017 for NavIC PRNs 2,5 and 6.

In order to characterize amplitude scintillation researchers used an $\alpha - \mu$ distribution which in general is a fading model, which explores the non-linearity of the propagation medium and a revised form of the Stacy (generalized Gamma) distribution was proposed[10]. The model is described by the coefficients α and μ of the normalised amplitude envelope of the received signal(r), where α is the modulus of sum of the multipath components and μ is the number of multipath components and the $alpha - mu$ probability density function, assuming that the average signal power (or intensity) r^2 is equal to 1 for $E[R^2] = 1$ is defined as[11]:

$$f(r) = \frac{\alpha r^{\alpha\mu - 1}}{\zeta^{\alpha\mu/2}\Gamma(\mu)} exp\left(-\frac{r^{\alpha}}{\zeta^{\alpha/2}}\right), \tag{1}$$

where

$$\zeta = \frac{\Gamma(\mu)}{\Gamma(\mu + 2/\alpha)} \tag{2}$$

in which $\Gamma(.)$ is the gamma function. S_4 index characterizes the strength of amplitude scintillation where the intensity of received signal $I = |r^2|$. The Nakagami-m parameter in the Nakagami distribution can be related to S_4 index by the following notation where $m = 1/S_4^2$ and the relation to estimate this is given below[11]

$$m = \frac{E^2(r^2)}{E(r^4) - E^2(r^2)} \tag{3}$$

$$\frac{E^2(r^{\beta})}{E(r^{2\beta}) - E^2(r^{\beta})} = \frac{\Gamma^2(\mu + \beta/\alpha)}{\Gamma(\mu)\Gamma(\mu + 2\beta/\alpha) - \Gamma^2(\mu + \beta/\alpha)} \tag{4}$$

By comparing Eq.4 with Eq 7, the left-hand side of equation (4) can be derived from field data for randomly chosen values of the parameter β, which provides the order of system of r to be determined. In fact, when the left-hand side of equation (4) for $\beta = 2$ is compared to the right-hand side of equation, the following results are obtained[11, 12]:

$$S_4{}^2 = \frac{\Gamma(\mu)\Gamma(\mu+4/\alpha) - \Gamma^2(\mu+2/\alpha)}{\Gamma^2(\mu+2/\alpha)} \quad (5)$$

If $\alpha = 2$ in the above equation (5) and the properties of the gamma function are used, the value of the left hand side of the same equation implies $1/\mu = 1/m$, which is the condition for the Nakagami-m distribution.

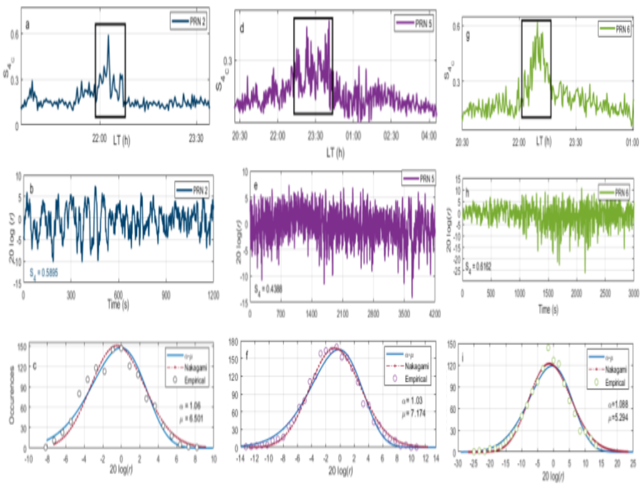

Figure 4. Intensity fading occurrences along with the $\alpha - \mu$ distributions and the Nakagami-m distribution as observed by NavIC PRNs' over Indore on September 8, 2017.

During the S_{4_c} event of September 8, 2017, the C/N_0 value of the NavIC PRNs' has significantly dropped below the range of 30 dB-Hz and have approached to zero between 22:00 to 0:00 LT (h) as observed from both the locations. The corresponding signal intensity fading (20log(r)) for Indore NavIC during the C/N_0 drop period, lasted for time period of 1200, 4200 and 3000 seconds for NavIC PRNs' 2, 5 and 6 respectively. The same intensity fading in case of Hyderabad NavIC PRNs'2, 5 and 6 lasted for about 4000, 2000 and 3000 seconds each. The S_{4_c} index as a function of local time is shown for each of the frequency in figures 4 and 5 (a,d and g) respectively, where the amplitude scintillation peaks are marked (in rectangular box) to indicate the fading sample that is used to calculate the signal intensity fading (20log(r)) as a function of time in seconds in figure 4 and 5 (b,e and h). The corresponding values of $\alpha - \mu$ and Nakagami distribution for the occurrences as a function of 20 log(r) is shown in figures 4 and 5 (c,f and i) for NavIC PRNs' 2, 5 and 6 as observed from Indore and Hyderabad respectively. The sample windows in the above observations and corresponding figures 4 5 show how the severity of fading occurrences increase as the value of S_{4_c} rises. The results for the values of $\alpha - \mu$ parameters also show that α increases with the increase in S_{4_c}

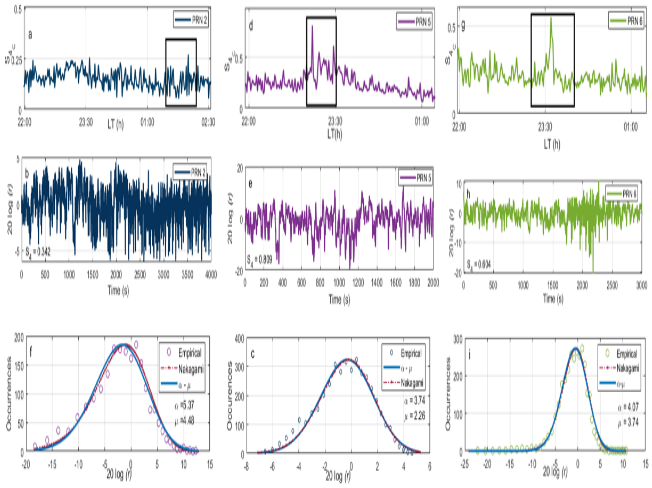

Figure 5. Intensity fading occurrences along with the $\alpha - \mu$ distributions and the Nakagami-m distribution as observed by NavIC PRNs' over Hyderabad on September 8, 2017.

5 Conclusions

A systematic study over the variable low-latitude region surrounding the EIA and the magnetic equator is essential to understand the low latitude and equatorial ionosphere. A study using NavIC, for the first time, under low solar activity conditions is presented here. Our work demonstrates how difficult it is for the receiver to retain lock as signal quality degrades. As a result, defining the statistics of these fades is crucial for estimating the effects of these phenomena and aid in the development of processing techniques and positioning algorithms that will reduce these effects in the receiver.

6 Acknowledgements

DA acknowledges the INSPIRE fellowship from the Department of Science and Technology, which she used to pursue her research. The authors also thank SAC, ISRO for providing the NavIC ACCORD receiver to the Department of Astronomy, Astrophysics, and Space Engineering, IIT Indore, under the NGP-17 project. The authors wholeheartedly thank Dr. P. Naveen Kumar for providing NavIC Osmania University (OU) Hyderabad station's data.

References

[1] Aarons, J., 1993. The longitudinal morphology of equatorial f-layer ir-regularities relevant to their occurrence. *Space Sci. Rev.*, **63**,209–243.doi:10.1007/BF00750769

[2] Ayyagari, D., Chakraborty, S., Das, S., Shukla, A., Paul, A., Datta,A., 2020. Performance of NavIC for studying the ionosphere at an EIA region in India. *Advances in Space Research* **65**, 1544 – 1558. doi:10.1016/j.asr.2019.12.019

[3] Taylor, S., Morton, Y., Jiao, Y., Triplett, J., Pelgrum, W., 2012. An improved ionosphere scintillation event detection and automatic trigger for GNSS data collection systems. *Proc ION ITM* , 1563–1569.

[4] Jiao, Y., 2013. High latitude ionosphere scintillation characterization. Dept. of Electrical and Computer Engineering, Univ Oxford Miami Ohio.

[5] Pi, X., Mannucci, A., Lindqwister, U., Ho, C., 1997. Monitoring of global ionospheric irregularities using the worldwide GPS network. *GeophysicalResearch Letters* **24**, 2283–2286.

[6] Ghosh, P., Otsuka, Y., Mani, S., Shinagawa, H., 2020. "Day-to-day variation of pre-reversal enhancement in the equatorial iono-sphere based on gaia model simulations.", *Earth, Planets and Space* **72**, 93. doi:10.1186/s40623-020-01228-9.

[7] Sousasantos, J., de Oliveira Moraes, A., A.Sobral, J.H., Muella, M.T.A.H.,de Paula, E.R., Paolini, R.S., 2018. "Climatology of the scintillation onsetover southern brazil", *Ann. Geophys*. **36**, pp 565–576. doi:10.5194/angeo-36-565-2018.

[8] Zou, Y., Wang, D., 2009. "A study of gps ionospheric scintillations observed at guilin.", *Journal of Atmospheric and Solar-Terrestrial Physics*, **71**, pp 1948–1958, doi:10.1016/j.jastp.2009.08.005.

[9] Liu, K., Li, G., Ning, B., Hu, L., Li, H., 2015a. "Statistical characteristics of low-latitude ionospheric scintillation over china.", *Advances in Space Research*, **55**, pp 1356–1365, doi:10.1016/j.asr.2014.12.001.

[10] Yacoub, M., 2007. 'The $\alpha-\mu$ distribution: A physical fading model for the stacy distribution.', *IEEE Trans. Veh. Technol.*, **56**, pp 27–34, doi:10.1109/TVT.2006.883753.

[11] Moraes, A., deMuella, M., deOliveira, C., Terra, W., Perrella, W., Meinbach-Rosa, P., 2017. 'Statistical evaluation of glonass amplitude scintillation over low latitudes in the brazilian territory.', *Adv Space Res*, **61**, pp 1776–1789, doi:10.1016/j.asr.2017.09.032.

[12] Humphreys, T., Psiaki M., Hinks, J., Kintner, P., 2009, "Simulating ionosphere-induced scintillation for testing gps receiver phase tracking loops.", *IEEE J Sel Top Signal Process*, **3**, pp 707–715. doi:10.1029/92RS01307.

[13] Tiwari, R., Strangeways, H., Tiwari, S., Ahmed, A., 2013, "Investigation ofionospheric irregularities and scintillation using tec at high latitude.", *AdvSpace Res.*, **52**, pp 1111–1124.

[14] Goswami, S., Paul, K., Paul, A., 2017, " Assessment of gps multi-frequency signal characteristics during periods of ionospheric scintillations from an anomaly crest location.", *Radio Science*, **52**, pp 1214–1222, doi:10.1002/2017RS006295.

[15] Moraes, A., dePaula, E. R. and Muella, M., Perrella, W., 2014, "On the second order statistics for gps ionospheric scintillation modeling", *Radio Sci*, **49**, pp 94–105, doi:10.1002/2013RS005270.

[16] Moraes, A., Paula, E., Perrella, W., Rodrigues, F., 2012, "On the distribution of gps signal amplitudes during the low-latitude ionospheric scintillation.", *GPS Solutions*, **17**, pp 499–510. doi:10.1007/s10291-012-0295-3.

A Calculating Amplitude Scintillation: S_{4_c} index, ROT, ROTI and Scattering Coefficients

The S_4 index is then calculated defined as the signal's normalised variance of intensity, which is expressed as[1, 7]:

$$S_4 = \sqrt{\frac{\langle {S_I}^2 \rangle - \langle S_I \rangle^2}{\langle S_I \rangle^2}} \tag{6}$$

where S_I is the intensity of the signal which is given as

$$S_I = 10^{0.1*C/N_0} \tag{7}$$

$$S_{AN} = \sqrt{\frac{100}{C/N_0}\left[1+\frac{500}{19C/N_0}\right]} \tag{8}$$

Now subtracting equation (8) from equation (6) the real estimate for S_{4_c} is obtained as shown below which is the ambient noise (S_{AN}) free index:

$$S_{4_C} = S_4 - S_{AN} \tag{9}$$

ROT and ROTI[13] values are calculated as given in equations below where in equation (10) $STEC_{r+1}$ and $STEC_r$ are slant TEC at *r+1* and *r* time epochs; Δt_r time interval; usually the unit of ROT is TECU/min and in equation (11) where $\langle ROT \rangle$ denotes averaging ROT during N epochs.

$$ROT = \frac{STEC_{r+1} - STEC_r}{\Delta t_r}. \tag{10}$$

$$ROTI = \sqrt{\langle ROT^2 \rangle - \langle ROT \rangle^2} \tag{11}$$

A scattering coefficient[14] across a pair of frequencies was later defined as the difference of $C/N0$ fluctuations normalised with respect to the amount of those fluctuations, based on these computed $C/N0$ deviations. The formula for scattering coefficient is given by (12) where a is the C/N_0 deviations calculated from one frequency is substituted and b is the C/N_0 deviations calculated from second frequency respectively. Here $S_{a,b}$ is a dimensionless quantity with values near zero suggesting good similarity between the signals.

$$S_{a,b} = \left[\frac{a-b}{a+b}\right] \tag{12}$$